JOURNAL OF COMPUTATIONAL PHYSICS 36, 417–427 (1980)

Note

Analysis of the Effect of Boundary Conditions on Numerical Stability of Solutions of Navier–Stokes Equations

The purpose of this note is to emphasize the cause of the computational instabilities of the ADI scheme. A heuristic extension of the Fourier method involving the effects of various types of boundary conditions is applied to two problems, the driven cavity flow and the natural convection in an inclined solar cell.

1. INTRODUCTION

When an ADI-type time marching procedure is used to solve the unsteady Navier–Stokes equations, it is well known [1] that numerical stability problems occur, although an unconditional stability is predicted by analysis using the conventional Fourier–Von Neumann method. As suggested by Roache [1], the lack of convergence may be due to non-linear instability for the interior points, or to the influence of the boundary conditions, which are not taken into account in this method.

The purpose of this note is to emphasize the cause of the computational instabilities. For this, an extension of the Fourier method involving various types of boundary conditions is applied to two problems. Such an extension, which has been similarly worked out by Taylor [2], and Trapp and Ramshaw [3], is only heuristic. But, as noted in Ref. [3], the conventional method is generally applied as a local method and is then also heuristic. In the case of a parabolic equation [3], the results obtained with this method have been shown to be very close to those obtained with more elaborate methods, such as the energy method. Another type of stability analysis, which is more complete than the Fourier method and which takes into account the boundary conditions, has been worked out by Smolderen [4]. In this last study, improvements have been made in the case of hyperbolic equations treated with an explicit scheme. They exhibit the influence of the boundary conditions on the generation of instabilities. In the case of the Navier–Stokes equations discretized with an ADI scheme, this type of stability analysis is not easy to apply, and the heuristic extension of the Fourier analysis has been preferred, as a first approach, to determine the stability conditions.

Some authors [2, 5–7] have previously mentioned from numerical experience that the boundary conditions imposed on the ADI scheme a time step restriction of the

0021-9991/80/090417-11$02.00/0

form $\Delta t/h^2 < a$. However, the applications were restricted to a limited range of flows and the investigation of the numerical stability was not sought systematically.

The present stability analysis has been used for the driven cavity problem and for the natural convection in an inclined solar cell, differentially heated. This study aims to derive stability criteria which involve the main parameters of these model problems, viz., the Reynolds number, Re (driven cavity problem), the Prandtl number, Pr, and the Rayleigh number, Ra (natural convection problem).

2. Governing Equations

The governing equations for these two problems are considered in a non-conservative form in vorticity, temperature, and stream function variables.

$$\zeta_t + u\zeta_x + v\zeta_y = a_1(\zeta_{xx} + \zeta_{yy}) + a_2(\sin \Omega \cdot T_y + \cos \Omega \cdot T_x), \tag{1a}$$

$$T_t + uT_x + vT_y = a_3(T_{xx} + T_{yy}), \tag{1b}$$

$$\psi_{xx} + \psi_{yy} = \zeta, \tag{1c}$$

where $u = \psi_y$ and $v = -\psi_x$.

In the case of the driven cavity [1, 8], the coefficients are $a_1 = 1/Re$, $a_2 = 0$ and, then, there is no need to solve the energy equation. In the case of the natural convection [9, 10], the coefficients are $a_1 = Pr$, $a_2 = Ra\ Pr$, and $a_3 = 1$, and Ω is the inclination angle measured from the horizontal.

In many applications, the boundary conditions on the variable ψ are overspecified: ψ and its first derivative normal to the wall, ψ_n, are given on each boundary (no-permeability and no-slip conditions). For the energy equation, the problem is well specified either by Dirichlet conditions or by Neumann conditions. However, concerning Eq. (1a), no physical condition exists for the vorticity at the boundaries, and ζ values are determined by an expansion procedure using the no-slip conditions. Second-order formulations are derived from Ref. [1]:

$$\text{Woods' formulation:} \quad \zeta_w = -\frac{1}{2}\zeta_{w-1} + \frac{3}{h^2}\psi_{w-1} - \frac{1}{h^2}\psi_w + \frac{3}{h}u_w, \tag{2a}$$

$$\text{Jensen's formulation:} \quad \zeta_w = \frac{1}{2h^2}(-\psi_{w-2} + 8\psi_{w-1} - 7\psi_w) + \frac{3}{h}u_w, \tag{2b}$$

where h is the spatial step size.

3. Numerical Scheme

The ADI method is described in the driven cavity case. The advancement over $2\Delta t$ is accomplished in two steps for the vorticity transport equation (1a),

$$\frac{\zeta^* - \zeta^n}{\Delta t} + u\zeta_x^n + v\zeta_y^* - \frac{1}{Re}(\zeta_{xx}^n + \zeta_{yy}^*) = 0, \tag{3a}$$

$$\frac{\zeta^{n+1} - \zeta^*}{\Delta t} + u\zeta_x^{n+1} + v\zeta_y^* - \frac{1}{Re}(\zeta_{xx}^{n+1} + \zeta_{yy}^*) = 0, \tag{3b}$$

where the superscripts (n) refer to time level.

The streamfunction equation (1c) is similarly solved as a time-dependent problem, with two fictitious time steps $\Delta\tau$,

$$\frac{\psi^{n+1,*} - \psi^{n+1,l}}{\Delta\tau} - (\psi_{xx}^{n+1,l} + \psi_{yy}^{n+1,*}) + \zeta^{n+1} = 0, \tag{4a}$$

$$\frac{\psi^{n+1,l+1} - \psi^{n+1,*}}{\Delta\tau} - (\psi_{xx}^{n+1,l+1} + \psi_{yy}^{n+1,*}) + \zeta^{n+1} = 0, \tag{4b}$$

where l is the iteration index. The first step $(n+1, l=0)$ is identical to step n. When the transient solution is sought, iteration to convergence is used at each step $(n+1)$. In the present study the steady solution is required and only one iteration is used with the parameter $\Delta\tau$ arbitrarily chosen equal to Δt.

The half-step $*$ has no physical meaning, but it is necessary to use a correct prescription of ζ^* on the boundaries compatible with ζ^n and ζ^{n+1} [11]. The spatial derivatives are discretized with a second-order, accurately centered scheme. The nonlinear coupling terms, u and v, are expressed at the middle point (i, j) of the "five-point" basic mesh shown in Fig. 1.

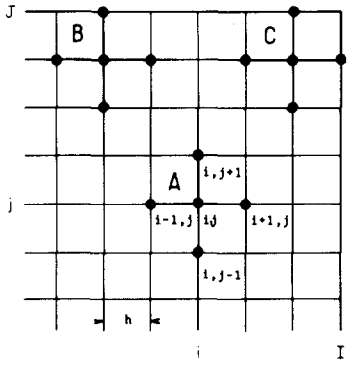

FIG. 1. Differencing mesh system: zero boundary point (case A); one boundary point (case B); two boundary points (case C).

4. Stability Analysis

The solutions of the discrete equations at the interior points are studied by using Fourier series expansions of components with separated variables,

$$\zeta_{ij}^n = Z^n e^{Im(i\theta_x + j\theta_y)}, \tag{5a}$$

$$\psi_{ij}^n = P^n e^{Im(i\theta_x + j\theta_y)}, \tag{5b}$$

where the subscripts (ij) refer to x, y indices $(1 < i < I,\ 1 < j < J)$. The solutions are considered locally at three points in each spatial direction. Three main cases are to be investigated (Fig. 1):

- — the conventional case, denoted (A), involving interior points only;
- — the case, denoted (B), where only one mesh point is on the boundary; (Associated conditions will be denoted "wall conditions.")
- — the case, denoted (C), where two mesh points are on the boundary. (Associated conditions will then be denoted "corner conditions.")

The linear coupled relations, either (2a) or (2b), are used as boundary conditions:

$$\zeta_{iJ}^n = \left(-\frac{1}{2} Z^n + \frac{3}{h^2} P^n\right) e^{Im(i\theta_x + (J-1)\theta_y)} + \frac{3u_{iJ}}{h}, \tag{6a}$$

$$\zeta_{iJ}^n = \frac{1}{2h^2} (8 - e^{-Im\theta_y}) P^n e^{Im(i\theta_x + (J-1)\theta_y)} + \frac{3u_{iJ}}{h}, \tag{6b}$$

with

$$\psi_{iJ}^n = 0. \tag{6c}$$

Relations (5), (6) are substituted into Eqs. (3), (4), which are solved as follows:

$$\begin{bmatrix} Z^{n+1} \\ P^{n+1} \end{bmatrix} = G \begin{bmatrix} Z^n \\ P^n \end{bmatrix} + C. \tag{7}$$

The necessary condition for the suppression of error amplification requires that

$$\text{Max} \, |\lambda_p| \leqslant 1, \tag{8}$$

where the λ_p are the eigenvalues of the matrix. The elements of G depend on the coefficients of the linearized systems, and in particular the coefficients u and v of the convective terms. Their importance will be shown later.

When the analysis is applied for system (3), (4) at interior points (case A), condition (8) is quite obviously shown to be always verified, which indicates unconditional stability. When it is applied in the neighborhood of the boundaries (cases B and C), the eigenvalues do not satisfy condition (8) for any value of the parameters. Then, one is interested in the study of the neutral stability conditions, that is,

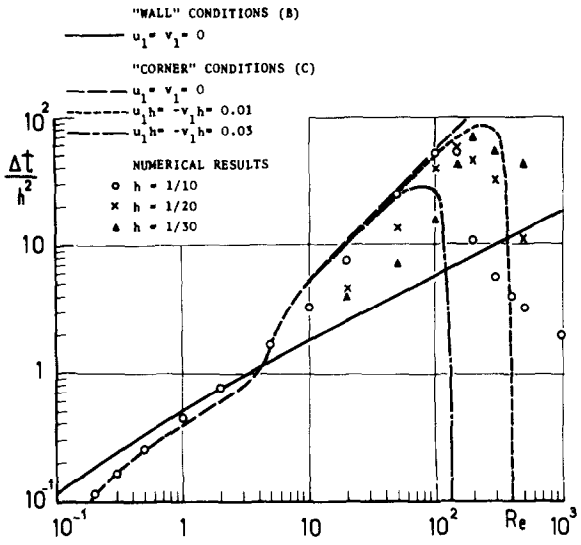

FIG. 2. Influence of Reynolds number on the numerical stability conditions (driven cavity).

Max $|\lambda_p| = 1$. Since G is only a (2×2) matrix, the eigenvalues are determined by a quadratic equation. The coefficients are complex and include the characteristic terms

$$u_1 \frac{\Delta t}{h}, \qquad v_1 \frac{\Delta t}{h}, \qquad \frac{1}{Re} \frac{\Delta t}{h^2},$$

where u_1 and v_1 are the values of u and v at the middle point of the mesh at the row adjacent to the boundary. They have, however, a quite complicated functional form; and it is then not possible to propose simple analytical relations between the parameters to characterize the neutral stability state. Such relations, which have the general form

$$F\left(u_1 \frac{\Delta t}{h}, v_1 \frac{\Delta t}{h}, \frac{1}{Re} \frac{\Delta t}{h^2}\right) = 0, \tag{9}$$

are determined "numerically" for each set of Re and h and for arbitrarily fixed u_1 and v_1 by calculating the associated Δt. The results are presented in Fig. 2. The solutions corresponding to $u_1 = v_1 = 0$ (Stokes problem) will be of significant interest and will be denoted Δt_{St} in further discussion.

5. DRIVEN CAVITY FLOW

The governing equations have been numerically integrated with the previously mentioned ADI technique by using the lagged Woods' estimate (2a) of the wall

values of ζ, i.e., $\zeta_w^{n+1} = \zeta_w^n$. For fixed values of Re, the behavior at convergence has been studied by varying Δt; when Δt is gradually increased from zero, the convergence is accelerated up to an optimum Δt value, beyond which the iterative process rapidly becomes non-convergent. The experimental critical values of Δt, denoted Δt_c, are presented in Fig. 2 versus Re for fixed values of h (disregarding the level of accuracy, which is indeed strongly dependent on Re).

For the case $u_1 = v_1 = 0$, the "wall" and the "corner" stability limits are the most restrictive conditions, respectively, for $Re \gtrsim 4$ and $Re \lesssim 4$, and, thus, should determine the overall stability.

First, we observe that the calculations are stable for $\Delta t_c/h^2$ larger than the predicted values (Fig. 2). Verification has been made that this might not be due to the fact that u_1 and v_1 are non-zero in practice. Indeed, when tested with the range of the calculated values of u_1 and v_1 for $Re > 4$, the resulting "wall" conditions appear, on the contrary, to be slightly more restrictive.

Second, we note that the experimental values $\Delta t_c/h^2$ are included between the "wall" and "corner" conditions $\Delta t_{st}/h^2$, as shown in Fig. 2, for $Re \lesssim 200$. When $Re \lesssim 4$, these two conditions are very close and allow a fairly precise prediction. When $200 \gtrsim Re \gtrsim 4$, they become substantially different; although it is less restrictive, the "corner" condition then appears to be a practical upper limitation for the numerical stability. Concerning this range of Re, the numerical results show that the experimental condition $\Delta t_c/h^2$ decreases from the "corner" condition, where $h = 1/10$, towards the "wall" conditions when the spatial step size is refined, as shown in Fig. 2 for $Re = 20$, 50, 100, and 150.

For $Re > 200$ and $h = 1/10$, the experimental values $\Delta t_c/h^2$ diverge from the predictions. Such a divergence has been conjectured to be connected to the influence of the coefficients u_1 and v_1 on the "corner" conditions. These coefficients become substantially different from zero for large Re. This fact is obvious in Fig. 2, which gives the predictions obtained with some arbitrarily fixed non-zero values of u_1 and v_1. These curves match the predictions $\Delta t_{st}/h^2$ for a wide range of Re values ($Re \lesssim 40$). When Re is further increased, these curves diverge from these predictions and finally exhibit a sharp decrease of $\Delta t_c/h^2$. The limiting values of Re have been found to correspond, then, to a cell Reynolds number limitation in the corner ($|u_1|\, Re\, h = 4$ or $|v_1|\, Re\, h = 4$). This cell Reynolds number limitation is half as restrictive as the one usually found in the literature for an explicit scheme [2]. It is, however, more restrictive than the empirical restriction on spatial mesh size mentioned by Torrance [6] for ADI scheme applied to flows characterized by diffusion coefficients nearing unity ($|u|\, h = 8$ or $|v|\, h = 8$). In addition, it is verified that the experimental values $\Delta t_c/h^2$ are again included between predictions $\Delta t_{st}/h^2$, when smaller step size values ($h = 1/20$, $h = 1/30$) are used. Moreover, this limitation on the size of h is not too restrictive, since it is also necessary to maintain accuracy through the boundary layer, in particular.

Furthermore, it is to be noted that the temporal and spatial step sizes used by Morris [7], with the same ADI scheme for (1a), agree also quite satisfactorily with our stability predictions, although (1c) is solved by a successive overrelaxation

TABLE 1

Morris Results ($Re = 100$)

h	1/14	1/16	1/32	1/56
$\Delta t/h^2$	49	40	48	28

routine and the evaluation of ζ_w used is the first-order-accurate Thom's equation [1]. These experimental conditions are shown in Table I for $Re = 100$ and for four values of h.

Obviously, then, it is of practical interest to obtain simple analytical expressions of these predictions in order to enclose the experimental stability conditions. For this purpose, approximate analytical formulae of F have been sought for the "wall" conditions (B) by considering the simplification $u_1 = v_1 = 0$; F is then written as

$$\text{when} \quad Re < \frac{1}{8}, \qquad \frac{\Delta t_{St}}{h^2} \simeq 2\,Re, \tag{10a}$$

$$\text{when} \quad Re > \frac{1}{8}, \qquad \frac{\Delta t_{St}}{h^2} \simeq \frac{1 + (1 + 24\,Re)^{1/2}}{12}. \tag{10b}$$

For the "corner" conditions (C), no simple analytical formulae have been found; therefore the following expressions of the critical values of Δt_{St} are obtained from curve fits to Fig. 2:

$$\text{when} \quad 0.20 < Re < 2, \qquad \frac{\Delta t_{St}}{h^2} \simeq 0.40\,Re^{0.60}, \tag{11a}$$

$$\text{when} \quad Re > 10, \qquad \frac{\Delta t_{St}}{h^2} \simeq 0.50\,Re. \tag{11b}$$

6. Natural Convection in a Solar Cell

When the natural convection is considered, the governing system involves the energy equation. The stability analysis is developed with one more variable, and the conditions are sought to be related to the physical parameters, Ra and Pr, under the form

$$F\left(u_1 \frac{\Delta t}{h}, v_1 \frac{\Delta t}{h}, Ra\,Pr \frac{\Delta t}{h}, Pr \frac{\Delta t}{h^2}\right) = 0. \tag{12}$$

Here, the Prandtl number, Pr, plays a role equivalent to the parameter $1/Re$ of the previous problem. The range of Prandtl number values considered in this study is

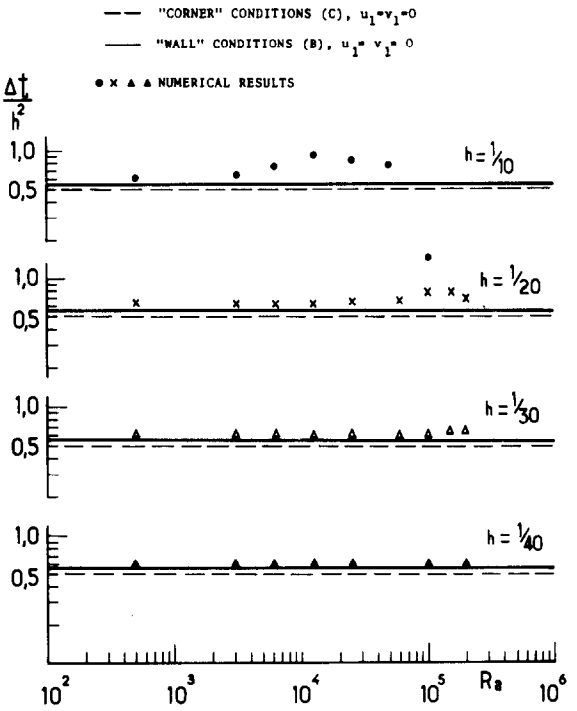

FIG. 3. Influence of Rayleigh number on the numerical stability conditions (solar cell, $Pr = 0.713$, $\Omega = 60°$).

from 0.1 to 10. The theoretical analysis of the stability has been investigated in the cases of the "wall" conditions (B) and the "corner" conditions (C).

One notes the presence of the Rayleigh number in (12), which couples momentum equations with the energy equation through the Archimedean forces. However, the conditions derived from the theoretical analysis of stability are predicted independently of *Ra*. This is confirmed by numerical experiments carried out by integrating the governing equations with Jensen's wall vorticity (2b), in the case of a solar cell (Fig. 3). The calculations concern a squared cell, at an inclination angle of 60°, for Rayleigh number values ranging from 500 to 200,000. For given values of *Ra* in this range, the effect of Δt on the rate of convergence of the ADI algorithm has been investigated up to a limiting value Δt_c, at which this algorithm breaks down. These critical experimental values Δt_c are shown in Fig. 3 and are in good agreement with theory (wall and corner conditions), especially when the step size h is small.

An analytical expression approximating the "wall" stability conditions has also been sought from (12) in the case $u_1 = v_1 = 0$, using Jensen's wall vorticity. This expression is written as

$$\frac{\Delta t_{St}}{h^2} \simeq \frac{1 + (1 + 28/Pr)^{1/2}}{14}. \tag{13}$$

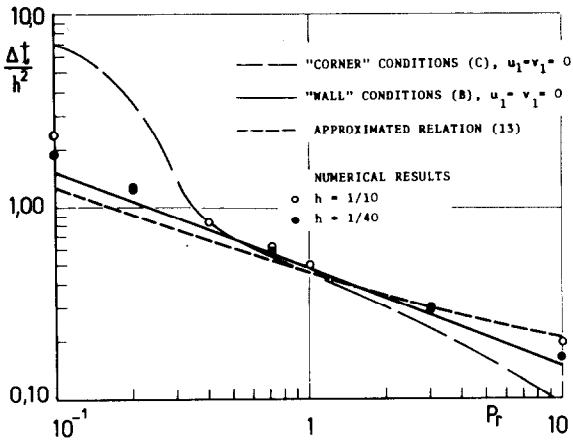

FIG. 4. Influence of Prandtl number on the numerical stability conditions (solar cell, $Ra = 500$, $\Omega = 60°$).

Condition (13) exhibits an effect of Pr which has been controlled for two step sizes when $0.1 < Pr < 10$ (Fig. 4). For the range of Prandtl number values, $Pr \gtrsim 0.4$, the agreement again appears to be entirely satisfactory between the values of Δt_c numerically tested for the "wall" stability condition (13). When $Pr \lesssim 0.4$, the Δt_c values diverge from this condition and, as previously observed for the driven cavity case, admit the corner conditions as an upper limit.

7. CONCLUSION

In conclusion, it appears that the heuristic extension of the Fourier analysis, including the effect of the boundary condition as proposed in the present paper, may allow the prediction of the breakdown of the ADI method used to solve numerically the two-dimensional Navier–Stokes equations. Criteria for the stability of this method have been derived in terms of the main physical parameters for problems as different as the motion in a driven cavity and the natural convection in a solar cell.

When the coefficient of the diffusive terms is large ($Re \lesssim 4$, $Pr \gtrsim 0.4$), the "corner" and "wall" stability criteria are slightly different and then give a rather precise prediction of the experimental condition. When the coefficient is small ($Re \gtrsim 4$, $Pr \lesssim 0.4$), the two predictions differ strongly; the "wall" criterion is the most restrictive and gives a lower limit for the experimental $\Delta t_c/h^2$, while the "corner" criterion gives an overestimation for these experimental values. Moreover, the reliability of the criteria (10), (11), (13), obtained in both these cases, is ensured when the cell Reynolds number is small near the corner, that is, when the spatial step size h is small enough. This last restriction is also imposed with respect to accuracy considerations.

APPENDIX: NOMENCLATURE

G	Amplification matrix
h	Spatial step size
n	Normal to the boundaries
P	Modulus of the Fourier component (5b)
Pr	Prandtl number
Ra	Rayleigh number
Re	Reynolds number
t	Time variable
T	Static temperature
u, v	Velocity components
u_1, v_1	Velocity component values at the discretized points in the neighborhood of the boundaries
x, y	Spatial variables
Z	Modulus of the Fourier component (5a)
$\Delta t, \Delta \tau$	Time step sizes
ζ	Vorticity
θ_x, θ_y	Phase angles
λ_p	Eigenvalue of the matrix G
ψ	Streamfunction
Ω	Inclination angle

Superscripts

l	Iteration index
n	Time index
*	Half-step for the ADI method
St	Stokes conditions defined in Section 4
c	Stability conditions from the numerical experiments
i, j	Spatial location index
w	Boundary conditions

ACKNOWLEDGMENTS

The research reported herein was supported in part by the Action Thematique Programmée n° 2988 of the Centre National de la Recherche Scientifique. The authors wish to acknowledge the contribution of R. Peyret, with whom they have had most fruitful discussions concerning this work.

REFERENCES

1. P. J. ROACHE, "Computational Fluid Dynamics," Hermosa, Albuquerque, 1972.
2. P. J. TAYLOR, *J. Comput. Phys.* **6** (1970), 268.
3. J. A. TRAPP AND J. D. RAMSHAW, *J. Comput. Phys.* **20** (1976), 238.

4. J. J. SMOLDEREN, Problèmes de stabilité numérique posés par les systèmes hyperboliques avec conditions aux limites, *in* "Lecture Notes in Computer Sciences, Vol. 11," pp. 135–159, Springer-Verlag, Berlin/New York, 1974.
5. N. R. BRILEY, "A Numerical Study of Laminar Separation Bubbles Using the Navier–Stokes Equations," Report J110614-1, United Aircraft Research Laboratories, East Hartford, Conn., 1970.
6. K. E. TORRANCE, *J. Res. Nat. Bur. Stand. B* **72**, No. 4 (1968), 281.
7. D. J. MORRIS, "Solution of the Incompressible Driven Cavity Problem by the Alternating Direction Implicit Method," pp. 47–59, NASA SP-378 (1975).
8. P. BONTOUX, B. FORESTIER, AND B. ROUX, *J. Mecan. Appl.* **2**, No. 3 (1978), 291.
9. G. K. BATCHELOR, *Quart. Appl. Math.* **12** (1954), 209.
10. J. C. GRONDIN, B. GILLY, P. BONTOUX, AND B. ROUX, Etude théorique du mouvement de convection naturelle dans une cavité rectangulaire inclinée, différentiellement chauffée, in preparation; Natural convection in inclined rectangular cells, *in* "Numerical Methods in Thermal Problems," pp. 423–432, Pineridge Press, Swansea, 1979.
11. G. FAIRWEATHER AND A. R. MITCHELL, *SIAM J. Numer. Anal.* **4** (1967), 163.

RECEIVED: November 22, 1977; REVISED: April 10, 1979

PATRICK BONTOUX*
BERNARD GILLY†
BERNARD ROUX‡

Institut de Mécanique des Fluides
1, rue Honnorat, 13003 Marseille, France

* Attaché de Recherche au CNRS.
† Professeur I.U.T. d'Aix-Marseille.
‡ Maître de Recherche au CNRS.